The Eurasia Proceedings of Science, Technology, Engineering & Mathematics (EPSTEM)
ISSN: 2602-3199

The Eurasia Proceedings of Science, Technology, Engineering and Mathematics (EPSTEM), 2025

Volume 37, Pages 163-179

ICEAT 2025: International Conference on Engineering and Advanced Technology

Numerical Investigation About Diesel Engine Powered by Waste Plastic Oil Blends Under Different Load and Engine Speed

Saif Aldeen Haider
University of Al-Qadisiyah

Mohamed F. Al-Dawody
University of Al-Qadisiyah

Abstract: The current study's objective is to use Diesel-RK simulation software to numerically assess the consequences of employing waste plastic oil blends on the thermal features of diesel engines. Each autonomous zone's governing equations are solved using the multi-zone combustion model. Three distinct volumetric blends were used to analyze the engine's characteristics of waste plastic oil (10 %, 20%, and 30 %) as a comparison to the standard diesel case with full and variable load and engine speeds. The data collected showed a slight decrease in the cylinder pressure for all blends at high engine speed compared to lower engine speed. The maximum value of BTE and heat release rate and lower BSFC accrue at 1500-2000 rpm. On the emissions side, a significant increase in the Bosch Smoke Number (BSN) was observed: 51.96%, 34.58%, 12.30%, and 0.012% at 1000 rpm, 1500 rpm, 2000 rpm, and 2500 rpm, respectively, compared to 3000 rpm for the 30% WPO at full load. A higher biodiesel content (30% WPO) resulted in a slight decrease in NO_x emissions compared to diesel at 3000 rpm. The findings suggest that 3000 rpm is recommended for fewer emissions and 1500-2000 rpm for higher BTE and less BSFC; the results are identical with other studies.

Keywords: Diesel-RK, Waste plastic oil (WPO), Diesel engine, NOx emissions, Numerical results, Thermal characteristics

Introduction

Since the industrial revolution in the late 18th and early 19th centuries, energy has been crucial for human progress and quality of life. This quest intensified due to the development of devices that convert energy into power(Knothe & Razon, 2017; Lin et al., 2011) An excellent example is the internal combustion engine, which comes in two main varieties: the compression-ignition (diesel) engine and the spark-ignition engine. The need for alternative energy sources has received a lot of attention lately because of the depletion of conventional fossil fuel supplies and growing environmental concerns. Additionally, some were drawn attention to biogenic materials, especially ethanol when it comes to SI engines (Kovarik, 1998) and, in the case of the CI engine, vegetable oils (Knothe, 2001), even though fuels derived from fossil fuels were studied from the beginning. There are four generations of biofuels (Mat Aron et al., 2020). In this article, we will discuss the fourth generation. Using photobiosolar fuel and electrical fuel as feedstock, fourth-generation biodiesel, and converting waste plastic are also branches of the fourth generation(Zhu et al., 2017). Although the biofuel produced from waste plastic is not a real biofuel like other generations, it is a link between the environmental problem resulting from waste plastic and converting it into useful energy. The waste plastic oil from the fourth generation of biofuel is extracted by using the pyrolysis method (Chang, 2023), while the other generations extract it by using the transesterification method (Li et al., 2019). The diversity in biofuel extraction methods results in variations in physical and chemical properties, but in general, biofuel has a greater viscosity and density and a lower heat content compared to fossil fuels (Murad & Al-Dawody, 2020). The chemical and physical personalities of biodiesel and diesel fuel are similar, according to several research studies (Demirbaş, 2002). Because of its fuel attributes and compatibility, biodiesel fuel research

is growing in popularity globally (Rao et al., 2017). Additionally, using biodiesel reduces the impact of greenhouse gases since it does not increase the quantity of carbon dioxide (CO_2) in the atmosphere(Singh & Singh, 2010). Also supports lower amounts of carbon monoxide, hydrocarbon, and smoke emissions(Chattopadhyay & Sen, 2013). Diesel engine performance is lower when using biofuel mixtures because the calorific value of biofuel is lower compared to diesel fuel and also has a higher fuel consumption rate. In this article, the use of waste plastic oil in a four-cylinder, two-stroke CI engine at variable engine speeds and variable loads will be discussed.

Materials and Methods

In this study, the use of oil mixtures produced from plastic waste will be discussed. For more knowledge on how to obtain waste plastic oil through the pyrolysis process, as in (Gao, 2010),. Diesel-RK has been developed with code that enables identification of the physical properties of various diesel oil mixtures, including RME, SME, and WPO. The software's potential as a competitive substitute for traditional diesel is demonstrated by the improved user interface that enables customers to personalize their desired biofuel-diesel mixes.

Waste Plastic Oil Preparation and Engine Test

The present research uses four test conditions—0%, 10 %, 20 %, and 30 % WPO blended with 100 %, 90 %, 80 %, and 70 % diesel, consequently, to examine the thermal properties of the diesel engine. The inquiry is predicated on a numerical simulation tool called Diesel-RK. Table 1 lists the qualities of the diesel and biodiesel that are being studied (Bharathy et al., 2019; Bhatt & Patel, 2022; Damodharan et al., 2017; D Damodharan et al., 2018; Dillikannan Damodharan et al., 2018; Kaimal & Vijayabalan, 2016; Kumar et al., 2020; Ma et al., 2017; Nalluri et al., 2023; Parthasarathy et al., 2021; Sachuthananthan et al., 2021; Sundar et al., 2022; Yaqoob et al., 2024). A Kirloskar TAF-1 type engine with a displacement volume of 661.45 cm^3 is employed. Table 2 illustrates the engine's specs.

Table 1. Diesel and WPO blends characteristics

Properties	Unit	Diesel	WPO 10%	WPO 20%	WPO 30%	Standard ASTM
C	%	87	86.89	86.77	86.66	_____
H	%	12.6	12.71	12.71	12.93	_____
O	%	0.4	0.402	0.41	0.41	_____
LHV	MJ/kg	45.84	45.29	44.74	44.19	D240
CN	_____	53.4	53.06	52.72	52.38	D976
Density @323K	kg/m^3	830.83	830.5	831	831.5	D1298
Kinematic viscosity	mm^2/s	2.7	2.68	2.67	2.65	D445
Molecular mass	g/mol	190	194.68	199.4	204	_____

Table 2. Information about the engine (Al-Dawody et al., 2023)

Engine Type	Kirloskar diesel engine
Type of product	TAF-1
Kind of engine	DI, 4-stroke, one-cylinder
Bore x Stroke	87.5 mm x 110 mm
Compression ratio	17.5
Rated power	4.41 kW
Cooling type	Liquid (water) cooling
Speed of the engine	1500 rpm
Injection type	Injecting directly
Injection pressure	160 bar
Diameter of nozzle	0.15 mm
Injection timing	20^o BTDC

Numerical Analysis

The Diesel-RK program was created by the Internal Combustion Engines department of Bauman Moscow State Technical University. It simulates engines in several modes and optimizes engine settings using mathematical models and algorithms. Additionally, it generates precise heat release rate graphs and 3D visualizations and

permits the usage of biofuels. This technique may also visualize spray evolution on a flat diagram using a 3D tool. The IC engine simulation's operational flowchart is displayed in Figure 1. For more details in (Noor & Hafizuddin, 2025)

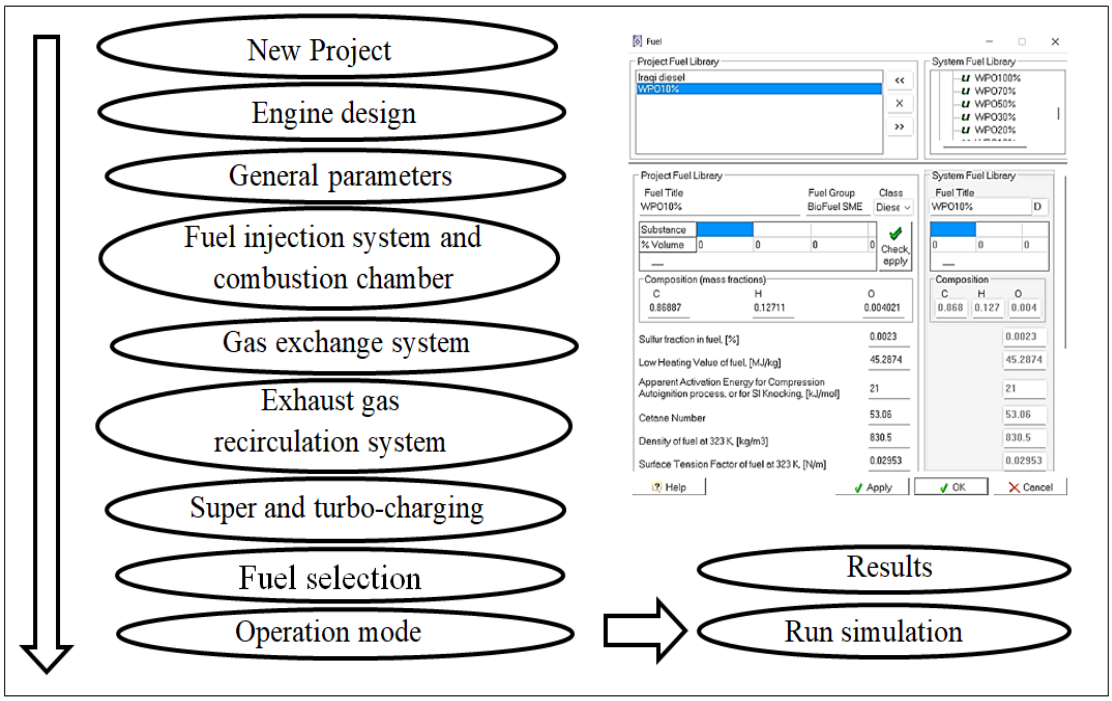

Figure 1. Operational flow chart for diesel RK software.

Two-stroke or four-stroke IC engines are evaluated and optimized using the Diesel-RK simulation tool, which belongs to a class of thermodynamic simulation programs.

- Conservation equations

$$\frac{dm}{dt} = \sum_i m_i \tag{1}$$

An open system's overall mass flow is preserved, as shown in equation (1) (Mohsen et al., 2023)

where m_i represents each species' mass flow rate. Equation shows the species conservation mathematical formula (2).

$$Y_{\mathrm{i}} = \sum_{\mathrm{i}} \frac{m_{\mathrm{i}}}{m} \tag{2}$$

where Yi stands for each species' mass fraction. Open thermodynamic systems can be represented using the following fundamental energy equation.

$$\frac{d(mu)}{dt} = -p\,\frac{dv}{dt} + \frac{dQ_{\mathrm{ht}}}{dt} + \sum_{\mathrm{i}} m_{\mathrm{i}} h_{\mathrm{i}} \tag{3}$$

Equation (3) shows the rate of energy change on the left, the displacement work and heat transfer rates on the right, and the entropy flow on the left.

- The spray evaluation model

According to reference Kuleshov (2005), A multi-area combustion prototype with fuel spraying is used in this investigation. Several different zones divide the fuel when it enters the combustion chamber. (Al-Dawody & Bhatti, 2013). An elementary fuel mass (EFM) moving quickly out of the injector to the end for spraying can be represented by the following statement:

$$[\frac{U}{U_0}]^{\frac{3}{2}} = 1 - \frac{l}{l_m} \quad (4)$$

Where:

U: An indicator for the elementary fuel mass current speed
U_0: The starting speed of the nozzle injector of the elementary fuel mass
l: the separation from the injector to the elementary fuel mass
l_m: the elementary fuel mass's penetration length till it comes to a halt ahead of a spray

A partial solution to the mathematical statement (1) may be found below. Figure 2 shows a simplified representation of the spray.

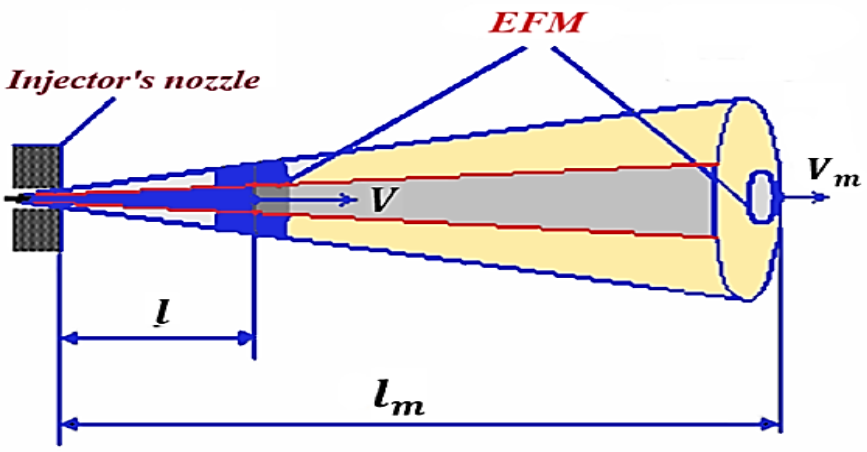

Figure 2. A spray nozzle design (Al-Dawody & Bhatti, 2013)

$$3l_m\left[-\left(1-\frac{l}{l_m}\right)^{0.333}+1\right]-U_o\tau_k = 0 \quad (5)$$

Where:

τ_k : Is the EFM's travel time proportional to the distance from the injector nozzle As the EFM of a spray tip stops, [$\tau_k = \tau_m$]
τ_m: Shows how long it takes for EFM to travel from the tip to the spraying head.

$$l_m = U_0\frac{\tau_m}{3} \quad (6)$$

Applying the formula (4) to (6)

The distance and current speed of EFM may be obtained as

$$U = U_o\left(1-\frac{\tau_k}{\tau_m}\right)^2 \quad (7)$$

$$l = \left[1-\left(1-\frac{\tau_k}{\tau_m}\right)^3\right]l_m \quad (8)$$

- Fuel allocation for spraying

A Diesel-RK combustion prototype divides the spraying into seven distinct zones, as shown in Figure 3. The requirements for burning and evaporation vary by zone. Prior to impingement of the jet during the free spray phase, only three zones need to be considered. Below is a list of some of these:

1. The free spray's thick conical center.
2. Thick in the free spray's tip.
3. Dilute the spray's outer sleeve.

4. NWF's thick conical nucleus.
5. Dense NWF on the piston surface
6. Congested NWF front.
7. NWF's diluted outer zone.

Calculating vaporized fuel is more challenging near the wall because of the heterogeneous flow. Therefore, in boundary flows, free spray measurements may be used to differentiate between mass, pattern areas, and heat transmission properties. Due to the effect with the wall, a fresh group of zones has to be assessed.

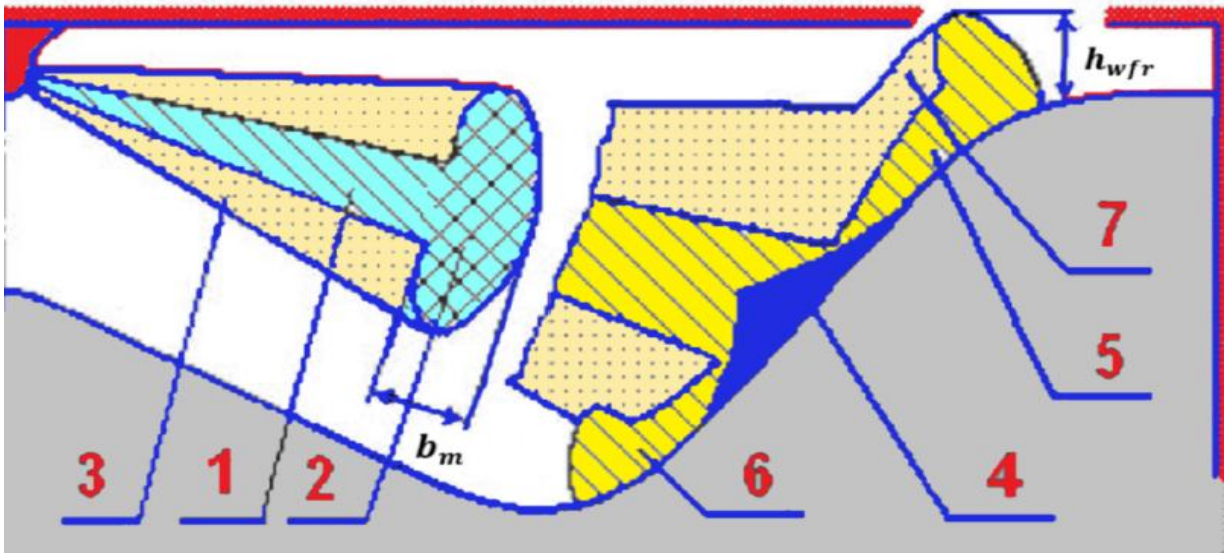

Figure 3. The spray fuel zones (Abdulwahid et al., 2023).

- Model of heat release:

Fuel typically burns in four phases, each of It possesses distinct chemical and physical features that limit how quickly it may burn (Edam & Al-Dawody, 2019; Murad & Al-Dawody, 2022).

a. Delay period

$$\tau = \sqrt{\frac{T}{P}} * e^{\left(\frac{E_a}{8{,}312T} - \frac{70}{CN+25}\right)} * 3.8 * 10^{-6} * (n * 1 - 1.6 * 10^{-4}) \quad (9)$$

where :

τ: Ignition delay second
T: Temperature in the cylinder
P: Current pressure in the cylinder Pa.
E_a: Apparente activation energy for the auto ignition process kJ/kmol

b. Premixed combustion phase

$$\frac{dx}{dt} = \varphi_1 \left\{\frac{d\sigma_u}{d\tau}\right\} + \varphi_o * \{A_o * (0.1\,\sigma_{ud} + x_o)(\sigma_{ud} - x_o)\left(\frac{m_f}{V_i}\right) \quad (10)$$

where:

σ_u : Fraction of the vapor formed during the ignition period. %
A_o : Constant .
x_o : Fraction of the fuel vapor formed during ignition delay and burnt out.
m_f : mass of fuel kg

c. Diffusion combustion

$$\frac{dx}{d\tau} = \{(\text{ø-}x)(\sigma_u - x) * \left\{\frac{m_f}{V_c}\right\} * A_2 \} * \varphi_2 + \left\{\frac{d\sigma_u}{d\tau}\right\} * \varphi_1 \quad (11)$$

where:

ø: Equivalence ratio.
x: fraction of heat release.
V_c : Cylinder volume m^3
A_2 : Constant

d. End of combustion

$$\frac{dx}{d\tau} = \varphi_3 A_3 K_T (1 - x)(\varepsilon_b \text{ ø-}x) \quad (12)$$

where:

K_T : Temperature in the related zone K
ε_b : Efficiency of air used %
A_3 : Constant

$\varphi_o = \varphi_3 = \varphi_2 = \varphi_1$ is a function that characterizes the areas' overall fuel vapor combustion.

- The growth of NO_x Modeling

The Zel'Dovich modified mechanism is used by the Diesel-RK software to characterize the NOx structure of diesel engines. Nitrogen dioxide and nitric oxide typically combine to produce NOx emissions (Kuleshov & Mahkamov, 2008). The nitrogen oxides (NOx) volume concentration was determined using an equation (13) (Al-Dawody et al., 2022):

$$\frac{d[NO]}{d\theta} = \frac{2.33*10^7 P.e^{-\frac{38020}{T_z}} [N_2][O]_e \left(1-\left(\frac{[NO]}{[NO]_e}\right)^2\right)}{RT_z\left[1+\left(\frac{2365}{T_z}\right)e^{\frac{3365}{T_z}} [NO]/[O_2]_e\right]} \left[\frac{1}{rps}\right] \quad (13)$$

NO: Oxides of nitrogen
T_z: Zonal temperature K

- Soot model

Particles of soot develop and oxidize as a result of the chemical process that takes place during combustion. When calculating the concentration of soot particles, it has a major impact on how polluted the environment is(Al-Dawody & Bhatti, 2013).

$$[C] = \int_{\theta_B}^{480} \frac{d[C]}{d\tau} \frac{d\theta}{6n} \left[\frac{0.1}{P}\right]^{\gamma} \quad (14)$$

Where [C] is the amount of soot in the cylinder currently.

The Bosch might be used in particle matter estimations (PM) emissions using the following calculation (15):

$$[PM] = 565 * [ln\frac{10}{10-Bosch}]^{1.206} \quad (15)$$

Validation

The simulation findings are verified by comparison with those of M. Mani et al. (Mani et al., 2011) in the manner shown in Figures 4 and 5. The database for application software employs the same operating circumstances and engine data. The engine's running conditions are shown in Table 3.

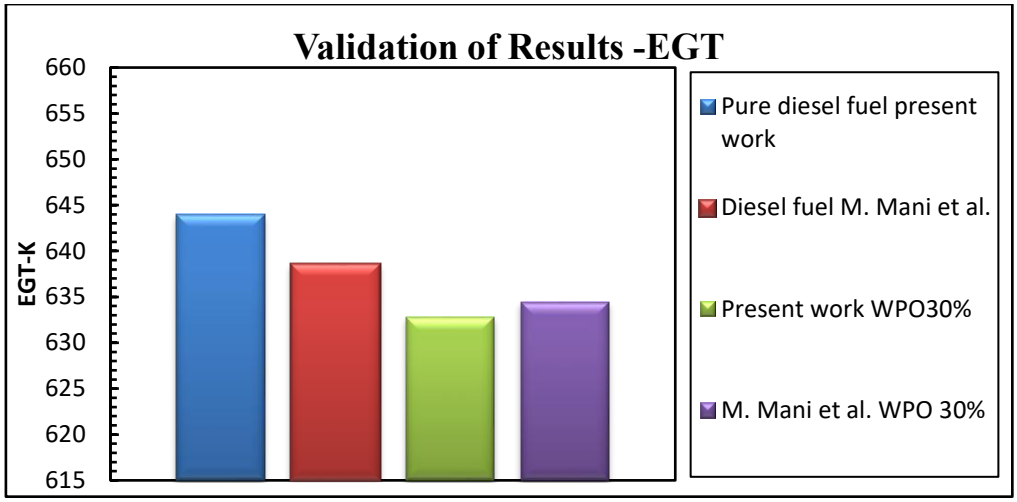

Figure 4. Exhaust gas temperature validation using additional research.

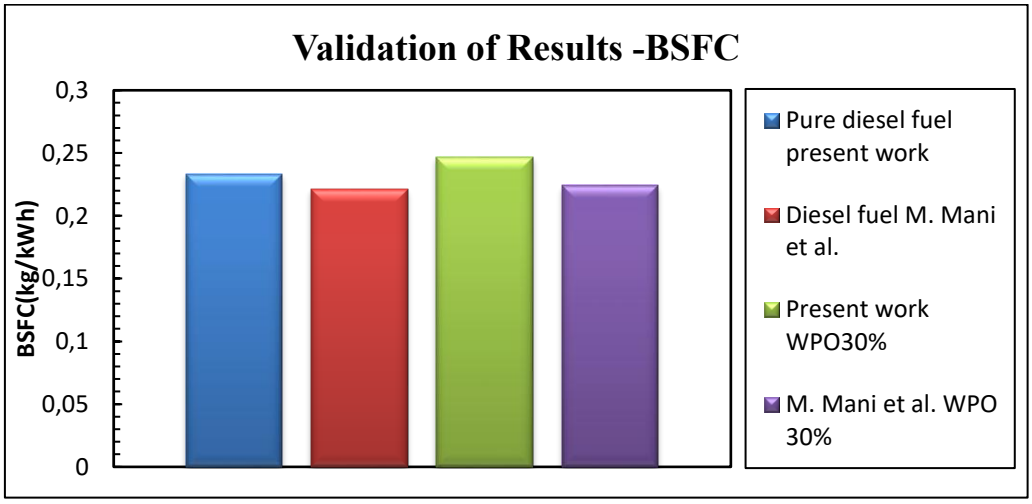

Figure 5. BSFC validation using additional research.

Table 3. Characteristics of the fuels that were utilized for validation.(Mani et al., 2011)

Characteristics	Units	waste plastic oil	Pure diesel
Density	Kg/m^3	840	840 to 880
Calorific value	(kJ/kg)	44340	46500
Kinematic viscosity	mm^2/sec	2.52	2.0
Cetane number	__	51	55
Sulphur Content	%	<0.002	<0.035
Flash Point	°C	42	50
Fire Point	°C	45	56
Aromatic content	%	55	20

These characteristics and specifications are now included in the program's fuels repository, as seen in Table 3 and Table 4, which display the engine parameters. When completely loaded, Figure 4 shows the diesel exhaust gas temperature data and 30% WPO. When using ordinary diesel, the study's variance is within 0.84 percent, and when using 30% WPO, it is within 0.25 percent. The BSFC values for pure diesel and 30% WPO at full operation load are displayed in Figure 5, and the findings are consistent with those of M. Mani et al.(Mani et al., 2011) are just 9% for the 30% WPO difference and 5% for diesel. It's important to keep in mind that the Diesel-RK program is a helpful and efficient modeling instrument tool that may simulate the combustion process of a diesel engine. An extra set of validations is produced by the tool to verify the results of other researchers. It uses the same setups and conditions inside its databases. These are compared with those produced in (Dasari et al., 2017; Prakash et al., 2018; Rajak et al., 2018) underneath the identical functioning conditions for the ongoing inquiry, using the same configurations and statuses in its databases. Table 5 contains the engines' technical specifications that were used for verification.

Table 4. Specifications of engine. (Mani et al., 2011)

Engine characteristic	Details
Model's make	Kirloskar TAF1
Type of Engine	4-stroke, CI, air cooled, 1-cylinder , DI diesel engine
Bore(cm)	8.75
Stroke (cm)	11
Compression ratio	17.5:1
Power rating at 1500 rpm (W)	4400
Nozzle opening pressure (MPa)	20
Retarded injection timing (°CA)	17° BTDC

Table 5. Characteristics of the three engine configurations utilized for verification (Dasari et al., 2017; Prakash et al., 2018; Rajak et al., 2018).

Test facility	Setup-1 Kirloskar	Setup-2 Kirloskar TV1	Setup-3 Legion Brothers
Kind of engine	4-stroke 1-Cylinder, Compression ignition engine	4-stroke 1-Cylinder, Compression ignition engine	4-stroke 1-Cylinder, Compression ignition engine
Bore x Stroke	8.75 cm x11 cm	8.75 cm x11 cm	8 cm x11 cm
Cooling system	Cooled by ail	Cooled by ail	cooled by water
Compression ratio	17.5:1	17.5:1	17.5:1
Rated power output	5148 W @ 1500 rpm	5200 W @ 1500 rpm	3700 W @1500 rpm
Injection pressure	20 MPa	16 MPa	20 MPa
Injection timing	23° BTDC	20° BTDC	23° BTDC

The engines are powered by ordinary diesel fuel. The pressure progression and the spray shape with the crank angle are shown in Figures 6 and 7. The analogy demonstrates a desired convergence with little change. There has been a little discrepancy noted. The low variance of Diesel-RK suggests that it is a trustworthy instrument for modeling how fuel is burned in internal combustion engines.

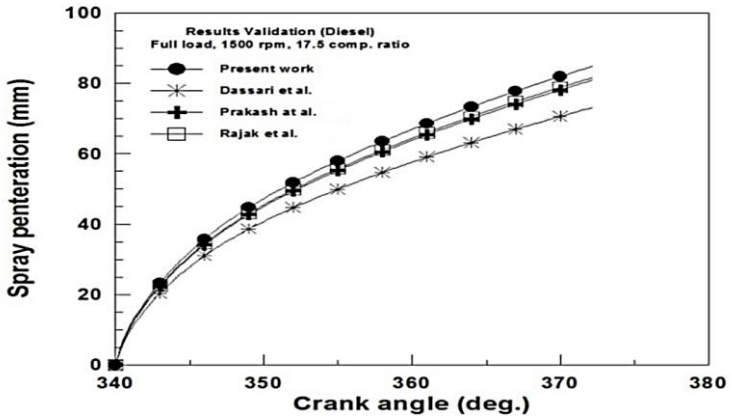

Figure 6. Spray dispersion versus crank angle validation.

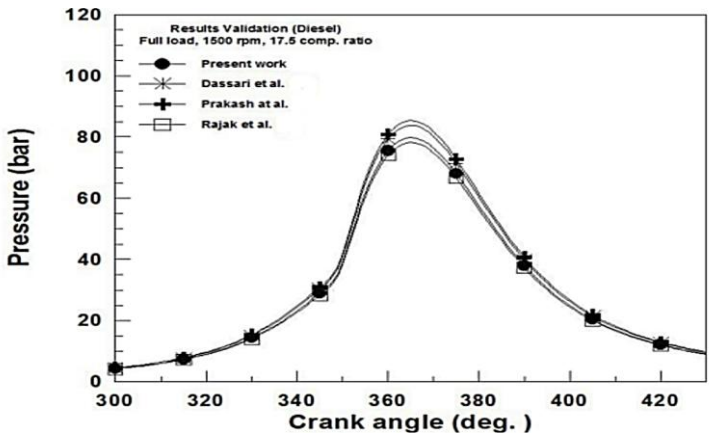

Figure 7. Cylinder pressure versus crank angle validation

Results and Discussion

Diesel-RK is a simulation program that is used to conduct the research. The variable load with the new scenario 'variable engine speed' is chosen to facilitate comparison of various blends regarding efficacy, combustion properties, and emissions of pollutants, also at full load, which is due to it having the lower air-to-fuel ratio. The following sections address the effects of WPO blends on associated performance, emission, and combustion characteristics.

Combustion Characteristics:

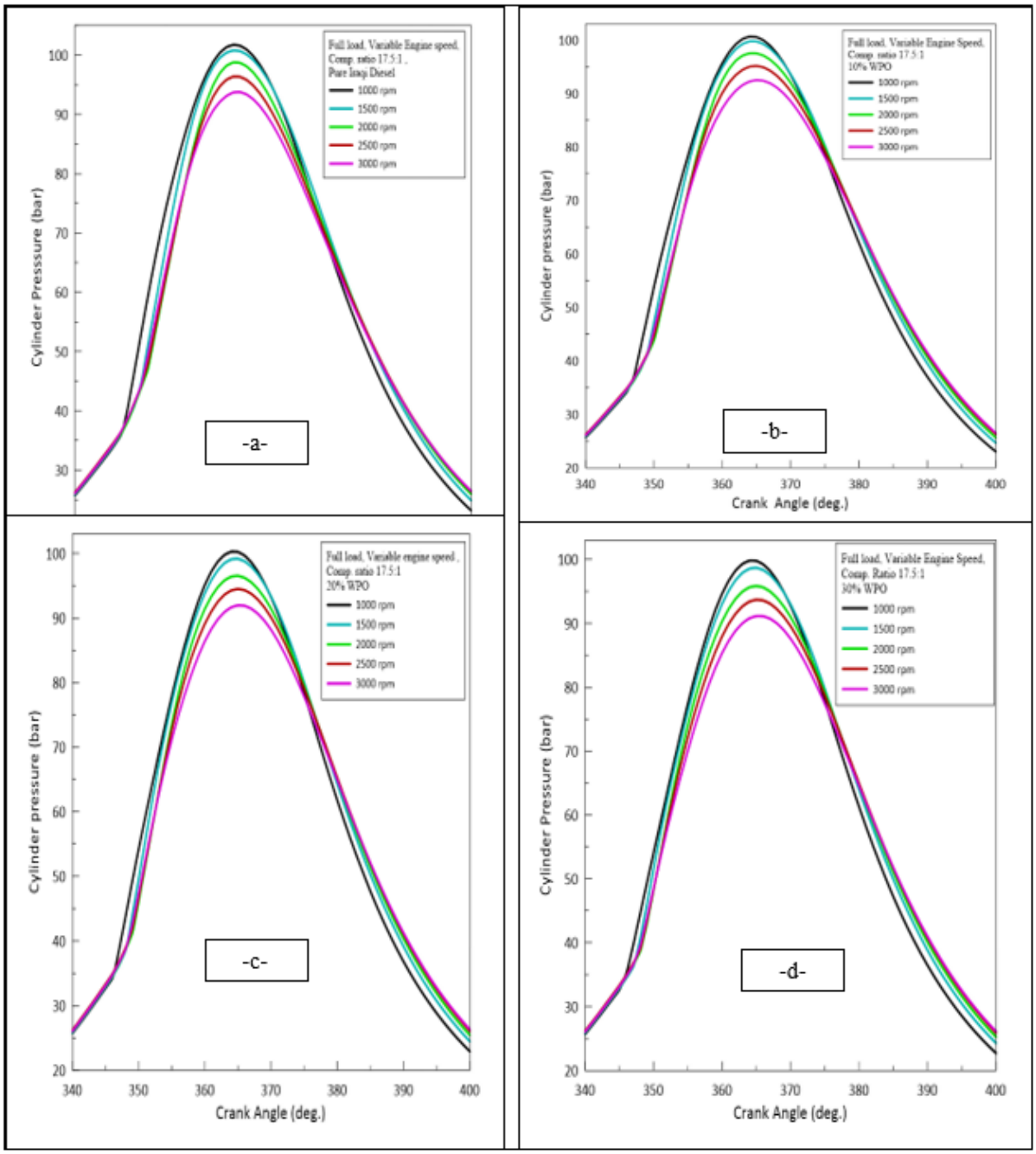

Figure. 8 (a,b,c,d). Cylinder pressure per crank angle at variable engine speed & full load

Figure 8 shows the pressure of the cylinder per crank angle at variable engine speed & full load, beginning at 180° BTDC and ending at 180° ATDC. This 360-degree phase is referred to as the power cycle, and it subsequently comprises compression, combustion, and expansion strokes. In general, the cylinder pressure of the biofuel is less

than that of fossil fuel. This is because the oxygen content is similar for both fuels, so the cylinder pressure is not affected. It is noted from the figures that the peak pressure reduces when the engine speed is increased. Peak pressure decreases as engine speed increases due to the poor burning rate of biodiesel fuels (Shehata, 2013). Peak pressure for pure Iraqi diesel decreased as engine speed increased, so the peak pressures for pure diesel at 1000 rpm, 1500 rpm , 2000 rpm, 2500 rpm, and 3000 rpm are 101.71 bar, 100.77 bar, 98.76 bar, 96.37 bar, and 93.75 bar. The peak pressures for the other blends, 10% WPO, 20% WPO, and 30% WPO, are 100.66 bar, 100.25 bar, and 99.79 bar, respectively, at 1000 rpm.

Figure 9 illustrates the variation in heat release within the 340°–385° crank angle range. The computational step considered is 0.2° crankshaft angle because major changes occur within this interval. Figure 9 presents the heat release rate of different blends at variable engine speeds. In general, the rate of heat release in WPO is less than pure diesel, and this is attributed to variations in viscosity, cetane number, and heating energy. The WPO blends have a later ignition start due to a lower cetane number.

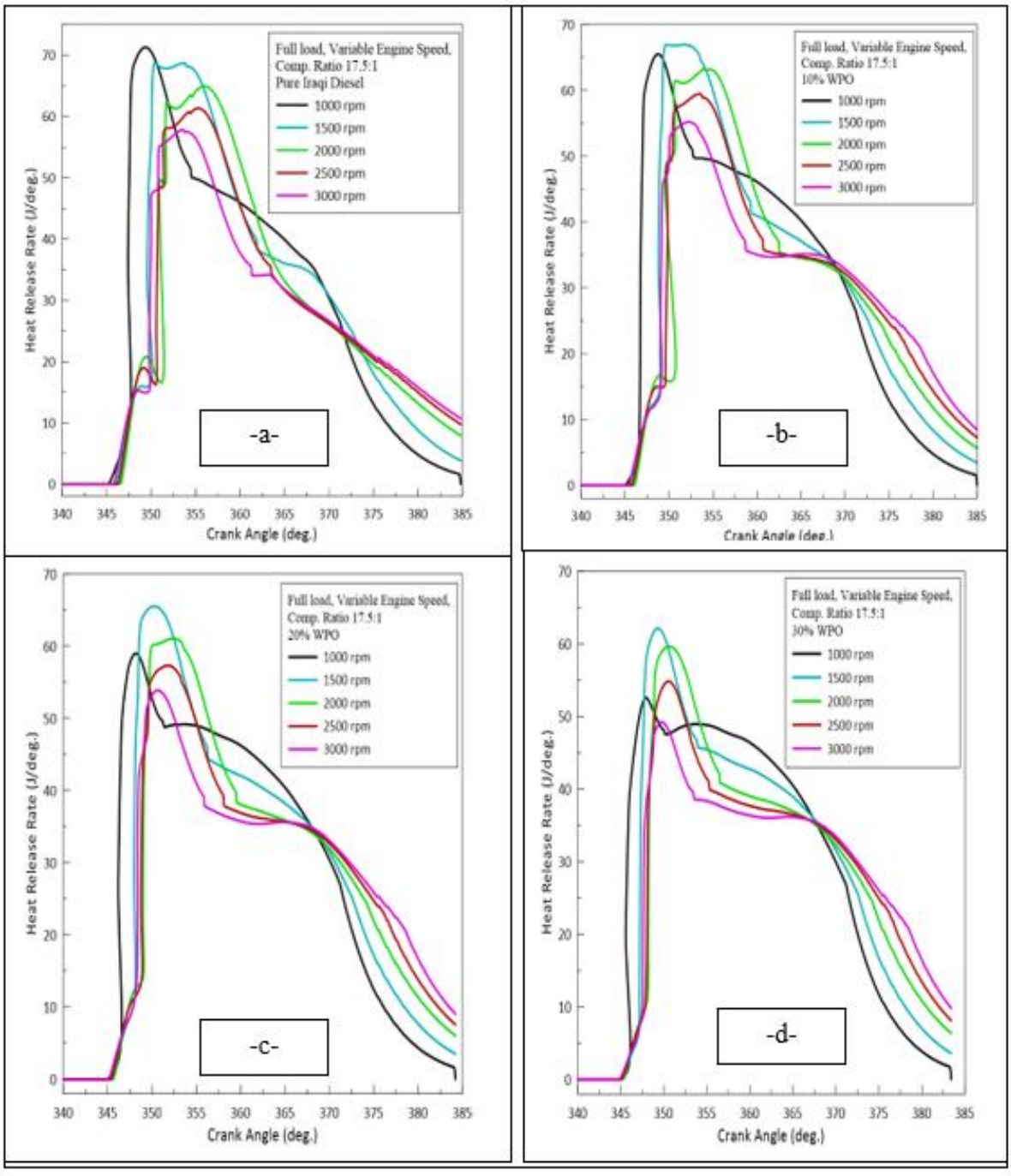

Figure 9 (a,b,c,d). Change of heat release rate with crank angle at full load and variable engine speed.

Figure 9a shows the change of pure Iraqi diesel with engine speed, and it notes that the HRR decreases with the rise of engine speed, so the maximum value accrues at 1000 rpm; it's 71.28 J/deg. at 349.4°. The other figures, b, c, & d, show the blends of WPO; the higher HRR for 10% WPO , 20% WPO, and 30% WPO accrues at 1500 rpm, equal to 66.93 J/deg., 65.55 J/deg., and 62.11 J/deg., respectively, and then reduces with the increase of engine speed. When engine speed increases, the start of combustion will be delayed further.

Performance Characteristics

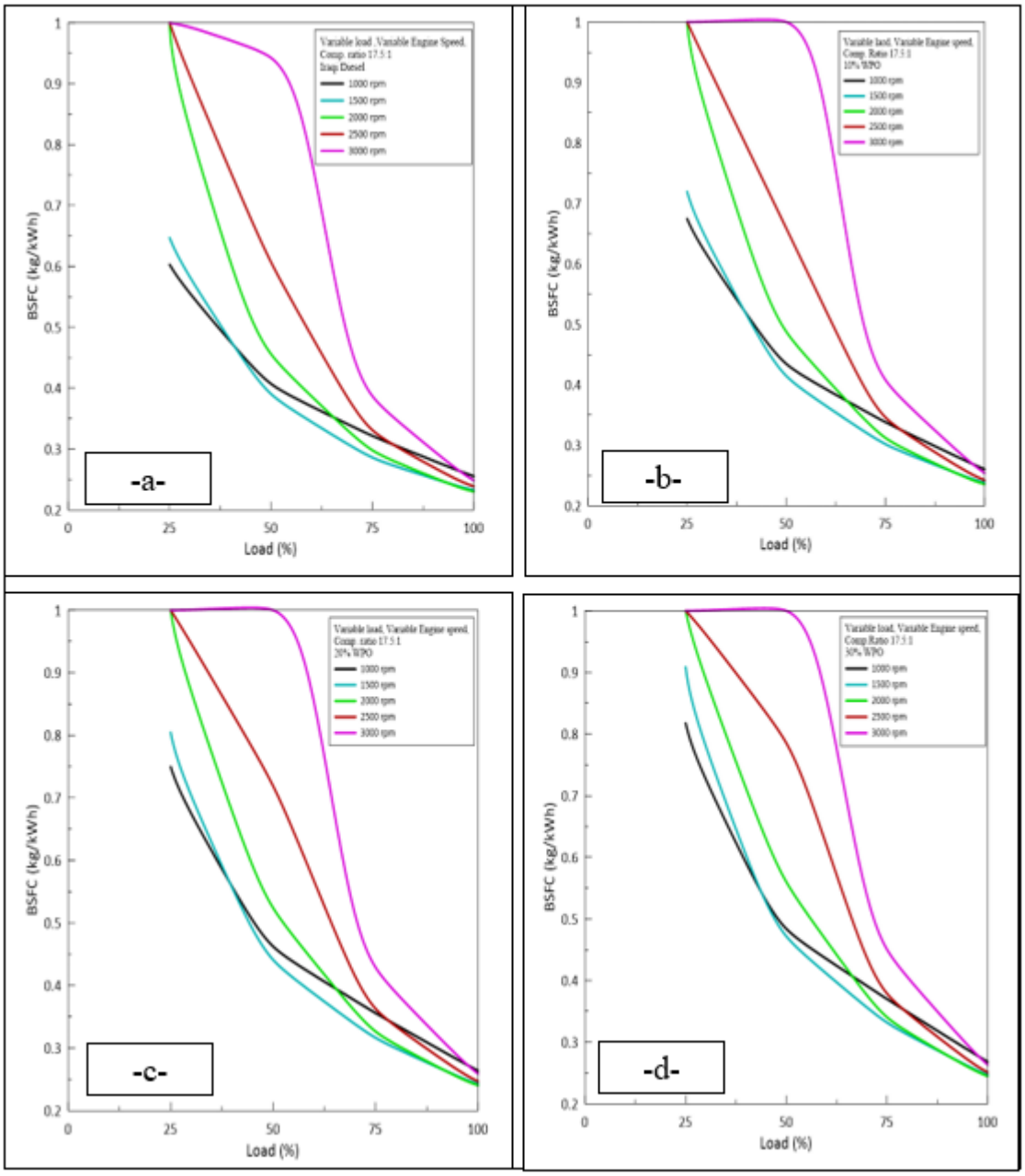

Figure 10 (a,b,c,d). The variation of BSFC with difference engine speed and difference load.

Figure 10 shows the variation of load for diesel and WPO blends. The BSFC decreases with the load increase. For different fuels, engine speed rises with fuel mass because of increased heat generation (Shehata, 2013). The BSFC for Iraqi diesel is 0.41 kg/kWh, 0.39 kg/kWh, 0.45 kg/kWh, 0.61 kg/kWh, and 0.94 kg/kWh for 1000 rpm, 1500 rpm, 2000 rpm, 2500 rpm, and 3000 rpm, respectively, at 50% load. The BSFC for 10% WPO, 20% WPO, and 30% WPO is 0.41 kg/kWh, 0.44 kg/kWh, and 0.47 kg/kWh for 50% load and 1500 rpm. In case of a full load, the results show that increasing the ratio of WPO in the mixture leads to a rise in the BSFC. This behavior is attributed to the LHV of the WPO fuel, which is distinctly lower than that of the pure diesel fuel (Abd Alla et al., 2002).

Therefore, more fuel must be added to the engine cylinder using WPO fuel for a certain target fuel energy input compared to diesel fuels (Devlin et al., 2008). From the simulation, it's noted that the minimum value of BSFC accrues at 2000 rpm and then rises with engine speed increasing. This is due to a lower air-to-fuel ratio at high speeds and a reduction in the volumetric efficiency of the engine. The same finding results in (Al_Dawody & Bhatti, 2014; Bayraktar, 2008; Sayin & Canakci, 2009)

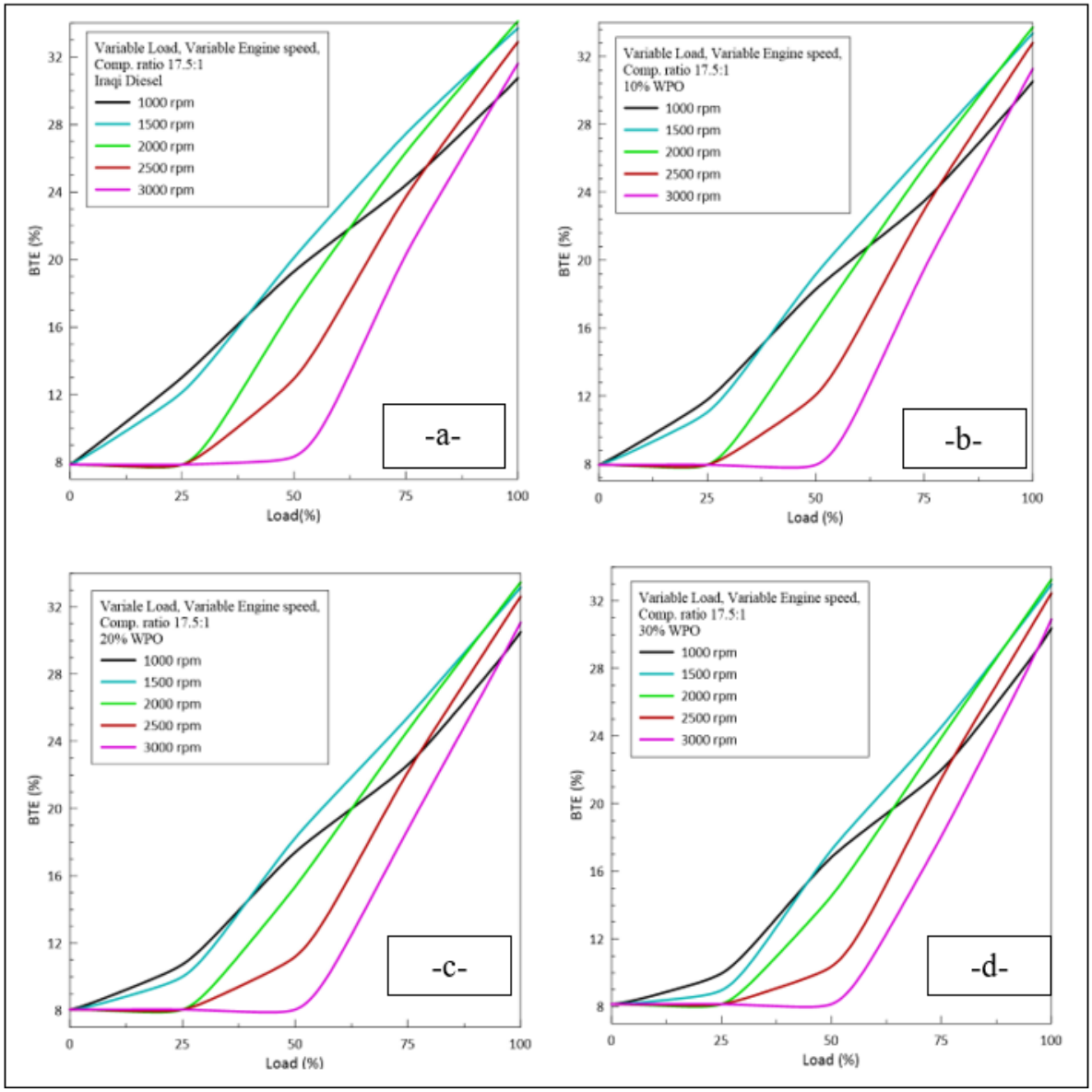

Figure.11 (a,b,c,d). Brake thermal efficiency with variable load and engine speed.

Figure 11 illustrates the impact of variable load and engine speed on diesel fuel and other mixtures. It shows that the BTE rate rises with increasing load and falls at high speeds; for all fuel types, the highest efficiency was observed at 1500 and 2000 rpm. The BTE value at 50% load was recorded for the 30% WPO at 16.83%, 17.263%, 14.54%, 10.37%, and 8.15% for 1000 rpm, 1500 rpm, 2000 rpm, 2500 rpm, and 3000 rpm, respectively, so the decreasing rate 0.86%, 2.43%, and 7.048% for 30% WPO at full load and at 1000 rpm, 1500 rpm, 2500 rpm, and 3000 rpm, respectively, compared to 2000 rpm. In case of a full load. The brake thermal efficiency (BTE) at full load and variable engine speed is higher for diesel fuel and other blends. 10% WPO, 20% WPO, and 30% WPO at 2000 rpm due to the variations in viscosity and density and low heating value for biofuel (Al_Dawody & Bhatti, 2014; Rajak et al., 2020) . It is also noticeable in the figure that the BTE value is low at very low and very high engine speeds. This can be explained by the fact that at high speeds combustion is incomplete due to the lack of air; the higher BTE accrues at 1500-2000 rpm at full load. The same finding results in (Chandra et al., 2011).

Emissions Characteristics

Figure 12 presents the variation of BSN with the variable load and engine speed. When load increase leads to an increase in BSN, but the increase in engine speed leads to a decrease in the value of BSN, it is 0.46, 0.26, 0.21, 0.15, and 0.12 for 1000 rpm, 1500 rpm, 2000 rpm, 2500 rpm, and 3000 rpm, respectively, at 50% load for Iraqi diesel. The maximum value of 50% load and 1000 rpm is 0.48, 0.44, and 0.40 for 10% WPO, 20% WPO, and 30% WPO at 50% load.

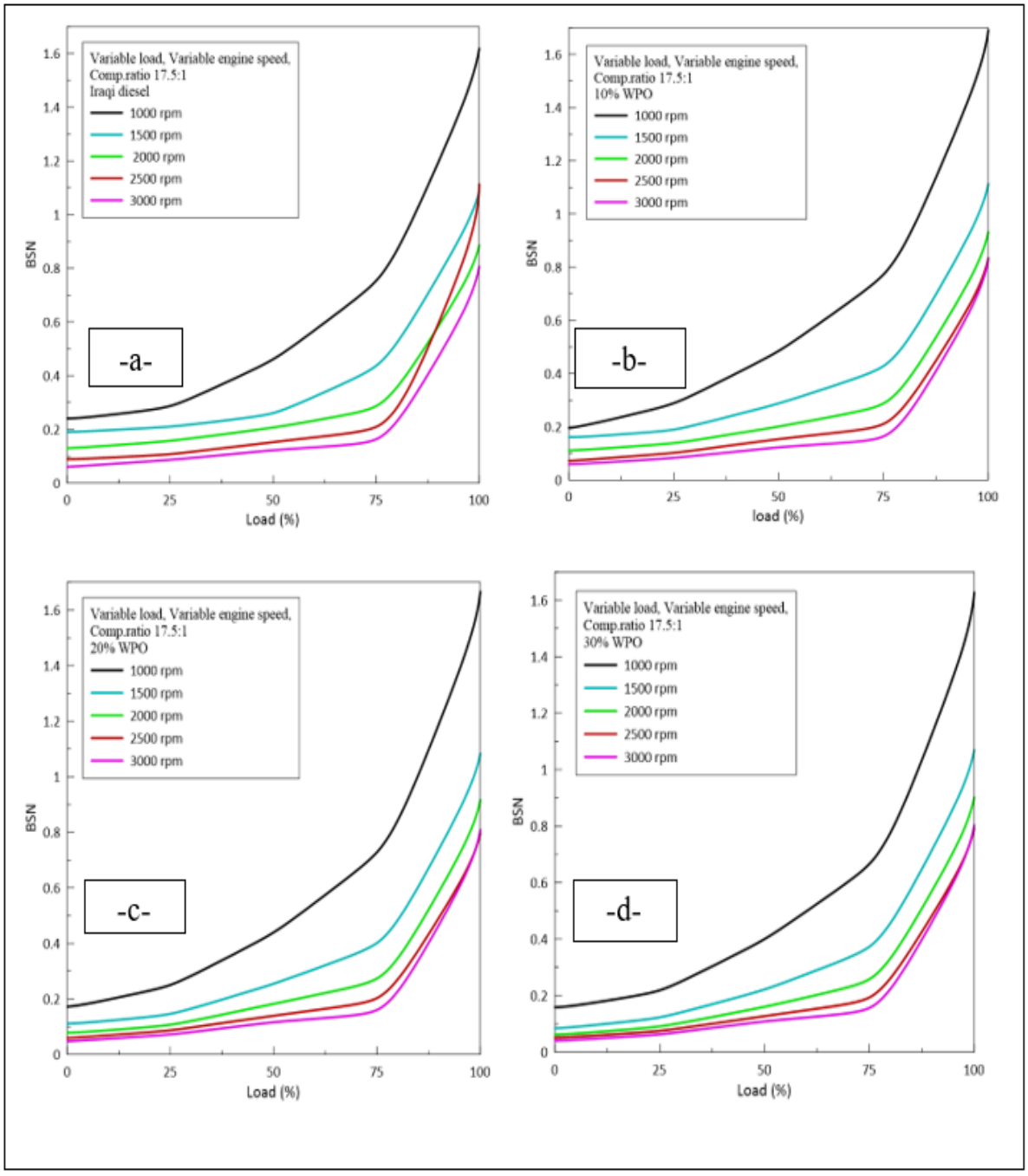

Figure 12 (a,b,c,d). Bosch smoke number with variable load.

In case of a full load, the use of waste plastic oil in general reduces the BSN where the reduction is compared with diesel fuel at an engine speed of 3000 rpm and a full load. It is noted that the BSN is also inversely proportional to the engine speed. The analysis of NOx with the variable engine speed and variable load is shown in Figure 13. It is clear that the emission rate is directly proportional to the load and inversely proportional to the engine speed. The decreasing rate of NOx at full load and maximum engine speed of 3000 rpm recorded for 1000 rpm, 1500 rpm, 2000 rpm, and 2500 rpm is 63.36%, 47.22%, 27.12%, and 11.26%, respectively, for 30% WPO.

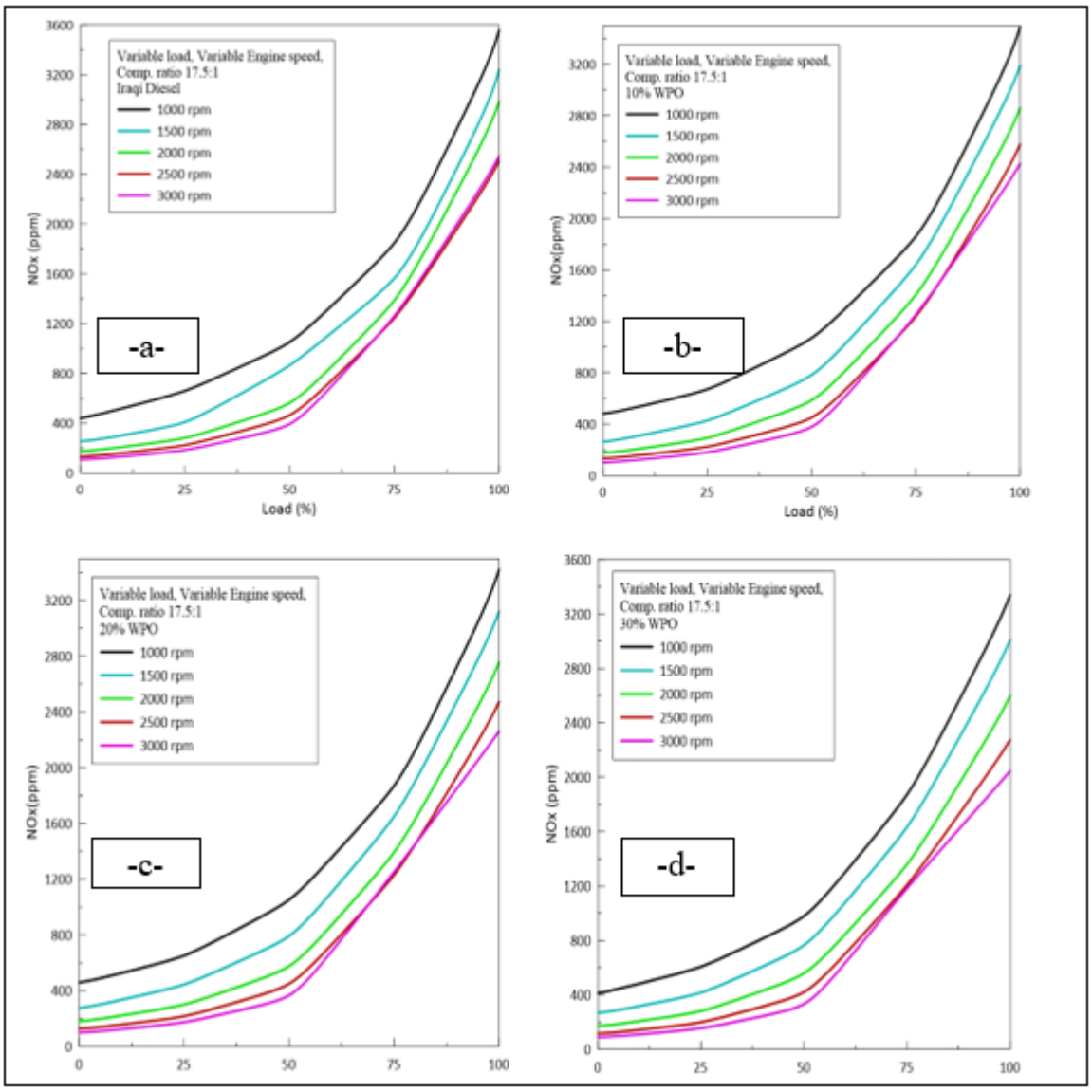

Figure13 (a,b,c,d). NO_x variation with variable load and engine speed.

In the case of full load and variable engine speed, the concentration of NOx for 30% WPO achieved the highest reduction in nitrogen oxide emissions at high speeds (3000 rpm). The percentage increase in nitrogen oxide emissions for pure diesel, 10% WPO, and 20% WPO compared to 30% WPO at 3000 rpm is recorded at 13.35%, 16.82%, and 9.19%, respectively. The reason for the decrease when increasing the engine speed may be due to a decrease in the maximum cylinder temperature.

Conclusions

The current study uses numerical analysis to examine the effects of three distinct volumetric mixes of waste plastic oil (WPO) biodiesel on diesel engine thermal parameters when compared to standard diesel operation. The current study came to the following conclusions:

1. WPO biodiesel is one potential tactic to cut down on diesel fuel consumption and address the rising levels of NO_x and carbon emissions.
2. Cylinder pressure, temperature, and heat release rate all slightly drop when WPO is blended with diesel.
3. The cylinder pressure reduces when the engine speed increases.
4. Higher BTE and lower BSFC occur at 1500-2000 rpm.
5. Maximum HRR accrues at 1500 rpm–2000 rpm, and it decreases when engine speed increases.

6. The temperature of exhaust gas increases, so it's recorded as 602.16 K, 632.91 K, 662.64 K, 690.31 K, and 723.27 K for 1000 rpm, 1500 rpm, 2000 rpm, 2500 rpm, and 3000 rpm for 30% WPO at full load.
7. It is recommended to conduct experimental research to examine how mixing WPO biodiesel affects the characteristics of diesel engines.
8. The results showed a sharp decrease in NOx emissions compared with diesel fuel at higher engine speeds.
9. To find out how the specified mixtures respond to different compression ratios, engine speeds, and injection timings, more optimization study is advised.
10. To investigate the real-world effects of WPO biodiesel blends on diesel engine characteristics, an experimental study is advised.

Scientific Ethics Declaration

* The authors declare that the scientific ethical and legal responsibility of this article published in EPSTEM journal belongs to the authors.

Conflict of Interest

* The authors declare that they have no conflicts of interest

Funding

* No funds have been allocated for this purpose.

Acknowledgements or Notes

* This article was presented as an oral presentation at the International Conference on Engineering and Advanced Technology (ICEAT) held in Selangor, Malaysia on July 23-24, 2025.

References

Abd Alla, G., Soliman, H., Badr, O., & Abd Rabbo, M. (2002). Effect of injection timing on the performance of a dual fuel engine. *Energy Conversion and Management, 43*(2), 269–277.

Abdulwahid, M. A., Al-Dawody, M. F., Al-Obeidi, W., Al-Farhany, K., Mohamed, M. H., Jamshed, W., Eid, M. R., & Alqahtani, H. (2023). Assessment of diesel engine thermo-characteristics working with hybrid fuel blends. *Numerical Heat Transfer, Part A: Applications, 84*(7), 659–674.

Al-Dawody, M. F., Al-Obaidi, W., Aboud, E. D., Abdulwahid, M. A., Al-Farhany, K., Jamshed, W., Eid, M. R., Raizah, Z., & Iqbal, A. (2023). Mechanical engineering advantages of a dual fuel diesel engine powered by diesel and aqueous ammonia blends. *Fuel, 346*, 128398.

Al-Dawody, M. F., & Bhatti, S. (2013). Optimization strategies to reduce the biodiesel NOx effect in diesel engine with experimental verification. *Energy Conversion and Management, 68*, 96–104.

Al-Dawody, M. F., Rajak, U., Jazie, A. A., Al-Farhany, K., Saini, G., Verma, T. N., & Nashine, P. (2022). Production and performance of biodiesel from *Cladophora* and *Fucus* green diesel. *Sustainable Energy Technologies and Assessments, 53*, 102761.

Al-Dawody, M. F., & Bhatti, S. (2014). Experimental and computational investigations for combustion, performance and emission parameters of a diesel engine fueled with soybean biodiesel–diesel blends. *Energy Procedia, 52*, 421–430.

Bayraktar, H. (2008). An experimental study on the performance parameters of an experimental CI engine fueled with diesel–methanol–dodecanol blends. *Fuel, 87*(2), 158–164.

Bharathy, S., Gnanasikamani, B., & Radhakrishnan Lawrence, K. (2019). Investigation on the use of plastic pyrolysis oil as alternate fuel in a direct injection diesel engine with titanium oxide nanoadditive. *Environmental Science and Pollution Research, 26*, 10319–10332.

Bhatt, V., & Patel, T. (2022, November). An experimental evaluation of emission characteristics of a single-cylinder diesel engine fuelled with waste plastic oil. In *International Conference on Science, Engineering and Technology* (pp. 25-26).

Chandra, R., Vijay, V. K., Subbarao, P. M. V., & Khura, T. K. (2011). Performance evaluation of a constant speed IC engine on CNG, methane enriched biogas and biogas. *Applied Energy, 88*(11), 3969–3977.

Chang, S. H. (2023). Plastic waste as pyrolysis feedstock for plastic oil production: A review. *Science of the Total Environment, 877*, 162719.

Chattopadhyay, S., & Sen, R. (2013). Fuel properties, engine performance and environmental benefits of biodiesel produced by a green process. *Applied Energy, 105*, 319–326.

Damodharan, D., Sathiyagnanam, A., Rana, D., Kumar, B. R., & Saravanan, S. (2017). Extraction and characterization of waste plastic oil (WPO) with the effect of n-butanol addition on the performance and emissions of a DI diesel engine fueled with WPO/diesel blends. *Energy Conversion and Management, 131*, 117–126.

Damodharan, D., Sathiyagnanam, A., Rana, D., Saravanan, S., Kumar, B. R., & Sethuramasamyraja, B. (2018). Effective utilization of waste plastic oil in a direct injection diesel engine using high carbon alcohols as oxygenated additives for cleaner emissions. *Energy Conversion and Management, 166*, 81–97.

Damodharan, D., Sathiyagnanam, A. P., Rajesh Kumar, B., & Ganesh, K. C. (2018). Cleaner emissions from a DI diesel engine fueled with waste plastic oil derived from municipal solid waste under the influence of n-pentanol addition, cold EGR, and injection timing. *Environmental Science and Pollution Research, 25*, 13611–13625.

Dasari, S. R., Chaudhary, A. J., Goud, V. V., Sahoo, N., & Kulkarni, V. (2017). In-situ alkaline transesterification of castor seeds: Optimization and engine performance, combustion and emission characteristics of blends. *Energy Conversion and Management, 142*, 200–214.

Demirbaş, A. (2002). Biodiesel from vegetable oils via transesterification in supercritical methanol. *Energy Conversion and Management, 43*(17), 2349–2356.

Devlin, C. C., Passut, C., Campbell, R., & Jao, T.-C. (2008). Biodiesel fuel effect on diesel engine lubrication. *SAE Technical Paper,* 0148-7191.

Edam, M. S., & Al-Dawody, M. F. (2019). Numerical simulation for the effect of biodiesel addition on the combustion, performance and emissions parameters of single cylinder diesel engine. *Al-Qadisiyah Journal for Engineering Sciences, 12*(2), 72-78.

Gao, F. (2010). *Pyrolysis of waste plastics into fuels. (*Phd Thesis). University of Canterbury.

Kaimal, V. K., & Vijayabalan, P. (2016). An investigation on the effects of using DEE additive in a DI diesel engine fuelled with waste plastic oil. *Fuel, 180*, 90–96.

Knothe, G., & Razon, L. F. (2017). Biodiesel fuels. *Progress in Energy and Combustion Science, 58*, 36–59.

Kovarik, B. (1998). Henry Ford, Charles F. Kettering and the fuel of the future. *Automotive History Review, 32*, 7–27.

Kuleshov, A. (2005). Model for predicting air–fuel mixing, combustion and emissions in DI diesel engines over whole operating range. *SAE Technical Paper* 0148-7191.

Kuleshov, A., & Mahkamov, K. (2008). Multi-zone diesel fuel spray combustion model for the simulation of a diesel engine running on biofuel. *Proceedings of the Institution of Mechanical Engineers, Part A: Journal of Power and Energy, 222*(3), 309–321.

Kumar, S. L., Radjarejesri, S., & Jawahar, R. R. (2020). Characterization of waste plastic oil as biodiesel in IC engines. *Materials Today: Proceedings, 33*, 833–838.

Li, P., Sakuragi, K., & Makino, H. (2019). Extraction techniques in sustainable biofuel production: A concise review. *Fuel Processing Technology, 193*, 295–303.

Lin, L., Cunshan, Z., Vittayapadung, S., Xiangqian, S., & Mingdong, D. (2011). Opportunities and challenges for biodiesel fuel. *Applied Energy, 88*(4), 1020–1031.

Ma, Y., Wang, Q., Sun, X., Wu, C., & Gao, Z. (2017). Kinetics studies of biodiesel production from waste cooking oil using $FeCl_3$-modified resin as heterogeneous catalyst. *Renewable Energy, 107*, 522–530.

Mani, M., Nagarajan, G., & Sampath, S. (2011). Characterisation and effect of using waste plastic oil and diesel fuel blends in compression ignition engine. *Energy, 36*(1), 212–219.

Mat Aron, N. S., Khoo, K. S., Chew, K. W., Show, P. L., Chen, W. H., & Nguyen, T. H. P. (2020). Sustainability of the four generations of biofuels – A review. *International Journal of Energy Research, 44*(12), 9266–9282.

Mohsen, M. J., Al-Dawody, M. F., Jamshed, W., El Din, S. M., Abdalla, N. S. E., Abd-Elmonem, A., Iqbal, A., & Shah, H. H. (2023). Experimental and numerical study of using LPG on characteristics of dual fuel diesel engine under variable compression ratio. *Arabian Journal of Chemistry, 16*(8), 104899.

Murad, M. E., & Al-Dawody, M. F. (2020, November). Biodiesel production from spirulina microalgae oil. In *IOP Conference Series: Materials Science and Engineering* (Vol. 928, No. 2, p. 022127). IOP Publishing.

Murad, M. E., & Al-Dawody, M. F. (2022). Effect of microalgae biodiesel blending on diesel engine characteristics. *Heat Transfer, 51*(7), 6616–6640.

Nalluri, P., Premkumar, P., & Sastry, M. C. (2023). Experimental study on a computerised VCR diesel engine running on oil made by pyrolyzing waste plastic using Red mud as a catalyst. *Green Analytical Chemistry, 5*, 100054.

Noor, C. W. M., & Hafizuddin, M. (2025). Analyzing the impact of various diesel types on the performance and emissions of marine diesel engines using Diesel-RK software. *Universiti Malaysia Terengganu Journal of Undergraduate Research, 7*(1), 16–26.

Parthasarathy, M., Ramkumar, S., Elumalai, P., Gupta, S. K., Krishnamoorthy, R., Iqbal, S. M., Dash, S. K., & Silambarasan, R. (2021). Experimental investigation of strategies to enhance the homogeneous charge compression ignition engine characteristics powered by waste plastic oil. *Energy Conversion and Management, 236*, 114026.

Prakash, T., Geo, V. E., Martin, L. J., & Nagalingam, B. (2018). Effect of ternary blends of bio-ethanol, diesel and castor oil on performance, emission and combustion in a CI engine. *Renewable Energy, 122*, 301–309.

Rajak, U., Nashine, P., Singh, T. S., & Verma, T. N. (2018). Numerical investigation of performance, combustion and emission characteristics of various biofuels. *Energy Conversion and Management, 156*, 235–252.

Rajak, U., Nashine, P., & Verma, T. N. (2020). Effect of spirulina microalgae biodiesel enriched with diesel fuel on performance and emission characteristics of CI engine. *Fuel, 268*, 117305.

Rao, K. P., Babu, T. V., Anuradha, G., & Rao, B. A. (2017). IDI diesel engine performance and exhaust emission analysis using biodiesel with an artificial neural network (ANN). *Egyptian Journal of Petroleum, 26*(3), 593–600.

Sachuthananthan, B., Krupakaran, R., & Balaji, G. (2021). Exploration on the behaviour pattern of a DI diesel engine using magnesium oxide nanoadditive with plastic pyrolysis oil as alternate fuel. *International Journal of Ambient Energy, 42*(6), 701–712.

Sayin, C., & Canakci, M. (2009). Effects of injection timing on the engine performance and exhaust emissions of a dual-fuel diesel engine. *Energy Conversion and Management, 50*(1), 203–213.

Shehata, M. S. (2013). Emissions, performance and cylinder pressure of diesel engine fuelled by biodiesel fuel. *Fuel, 112*, 513–522.

Singh, S., & Singh, D. (2010). Biodiesel production through the use of different sources and characterization of oils and their esters as the substitute of diesel: A review. *Renewable and Sustainable Energy Reviews, 14*(1), 200–216.

Sundar, S. P., Palanimuthu, V., Sathyamurthy, R., Hemalatha, D., Kumar, R. S., Bharathwaaj, R., Vasanthaseelan, S., & Chamkha, A. (2022). Feasibility study of neat plastic oil with TiO_2 nanoadditive as an alternative fuel in internal combustion engine. *Journal of Thermal Analysis and Calorimetry, 147*(3), 2567–2578.

Yaqoob, H., Tan, E. S., Ali, H. M., Ong, H. C., Jamil, M. A., & Farooq, M. U. (2024). Sustainable energy generation from plastic waste: An in-depth review of diesel engine application. *Environmental Technology & Innovation, 34*, 103467.

Zhu, B., Chen, G., Cao, X., & Wei, D. (2017). Molecular characterization of CO_2 sequestration and assimilation in microalgae and its biotechnological applications. *Bioresource Technology, 244*, 1207–1215.

Author(s) Information

Saif Aldeen Haider
University of Al-Qadisiyah, Department of Mechanical Engineering, Iraq
Contact e-mail: *saifaldeenhayder@qu.edu.iq*

Mohamed F. Al-Dawody
University of Al-Qadisiyah, Department of Mechanical Engineering, Iraq

To cite this article:

Haider, S A., & Al-Dawody, M. F. (2025). Numerical investigation about diesel engine powered by waste plastic oil blends under different load and engine speed. *The Eurasia Proceedings of Science, Technology, Engineering and Mathematics (EPSTEM), 37,* 163-179.